International Conference on Estuaries and Coasts
November 9-11, 2003, Hangzhou, China

3D SIMULATION OF FLOW AND POLLUTANT TRANSPORT IN THE SOUTH BRANCH OF THE CHANGJIANG ESTUARY

Zulin HUA, Xiabo LIU & Kejian CHU
College of Environment Science & Engineering, Hohai University,
Nanjing, 210098, China, Email:zulinhua@sina.com

Abstract: The Changjiang Estuary nearby Shanghai is one of the largest and the most complicated estuaries in China. The flow exhibits obvious 3D structure in the Changjiang Estuary due to the complex topography, tide and runoff, and the pollutant transportation is also complicated in the region. The south branch of the Changjiang Estuary is the main outfall channel to the East China Sea, and the runoff of south branch is about 95 percent of total runoff of the Changjiang Estuary. Based on POM Model, the three-dimensional flow and mass transportation mathematical model with an orthogonal curvilinear coordinate in the horizontal direction and sigma coordinate in the vertical direction for the south branch of the Changjiang Estuary is established in this paper. The basic equations are discretized by the finite difference method and the process splitting skill (the numerical computational process is divided to external mode and internal mode) is applied in this model. The computed range in south branch of the Changjiang Estuary is 91.70 kilometer in length and 1328.81 km^2 in area. The three dimensional flow field and polluted scope by Shidongkou waste discharge outlet of Shanghai city are simulated, and the computational results mimic the observed data well. This work is benefited for guidance of waste pollution control in the Changjiang Estuary.

Key words: Three-dimensional model; Changjiang estuary; South branch; Flow; Pollutant transport; Numerical calculation

1. INTRODUCTION

The Changjiang Estuary is the largest estuary in China, near by Shanghai−the largest city of China, and simultaneously the Changjiang delta region also is most developed economic area in China, not to mention Asia and the World. The Changjiang estuary is divided into south branch and north branch by Chongming Island. There are two islands of Changxing and Hengsha in the south branch (shown in Fig.3). Currently the south branch is main outfall channel to east China Ocean, and the south branch runoff is about 95 percent total flow discharge of the Changjiang Estuary. The runoff of the Changjiang Estuary is abundant, and the mean annual runoff is 29,500m^3/s. The annual distribution of runoff has obvious seasonal variation. The average discharge is 40,000m^3/s during flood period, and 18,000 m^3/s during drought period. The south channel of the Changjiang estuary becomes gradually wide in plane feature, and the reach is maximum wide-increased rate in Changjiang River. Moreover, the underwater topography is simultaneously changeful and complex. The Changjiang Estuary belongs to middle strength tidal estuary, and the tide is semi-diurnal. The average tidal range of Liuhekou observed station is 2.15m. The tidal period is 12h25min, in which the durations of flood tide and ebb tide are 8 hours 12 minutes and 4 hours 14 minutes respectively.

With the more increase of urban population and the economic boom along the south branch of the Changjiang Estuary, the problem of water body pollution is attached importance to by the government environment administration department. It is quite necessary to know the flow field and characteristic of pollutant transport in south branch the Changjiang Estuary. The flow exhibits obvious 3D structure due to the complex topography, tide and runoffs, and

the contaminant transport is more complicated in the region. In this paper, a three-dimensional flow and mass transport mathematical model for the south branch in the Changjiang Estuary is established. The three -dimensional flow field and the polluted scope of Shidongkou waste discharge outlet of Shanghai city are simulated.

2. 3D MATHEMATICAL MODEL

The three dimensional numerical model includes external mode and internal mode based on Princeton Ocean Model. The external mode is used to solve fast process for surface gravitational wave to gain water elevation and depth-averaged velocity, and the internal mode is applied to calculate slow process for gravitational wave to obtain the characteristic of the 3d velocity of *u, v*, *w* and pollutant concentration distribution.

2.1 BASIC EQUATIONS OF EXTERNAL MODE

Continuity equation:

$$h_1 h_2 \frac{\partial \eta}{\partial t} + \frac{\partial (h_2 U_1 D)}{\partial \xi_1} + \frac{\partial (h_1 U_2 D)}{\partial \xi_2} = 0 \tag{1}$$

Momentum equations:

$$\begin{aligned}
&\frac{\partial (h_1 h_2 D U_1)}{\partial t} + \frac{\partial}{\partial \xi_1}(h_2 D U_1^{\,2}) + \frac{\partial}{\partial \xi_2}(h_1 D U_1 U_2) + D U_2 (-U_2 \frac{\partial h_2}{\partial \xi_1} + U_1 \frac{\partial h_1}{\partial \xi_2}) \\
&= f h_1 h_2 U_2 D - g D h_2 \frac{\partial \eta}{\partial \xi_1} + h_1 h_2 [- < wu(0) + wu(-1) >] \\
&- \frac{g D h_2}{\rho_0} \int_{-1}^{0} \int_{\sigma}^{0} [D \frac{\partial \rho'}{\partial \xi_1} - \frac{\sigma' \partial D}{\partial \xi_1} \frac{\partial \rho'}{\partial \sigma}] d\sigma' d\sigma + \frac{\partial}{\partial \xi_1} [2 \overline{A}_M \frac{h_2}{h_1} \frac{\partial U_1}{\partial \xi_1}] \\
&+ \frac{\partial}{\partial \xi_2} [\overline{A}_M D \frac{h_1}{h_2} \frac{\partial U_1}{\partial \xi_2}] + \frac{\partial}{\partial \xi_2} [\overline{A}_M D \frac{\partial U_2}{\partial \xi_1}]
\end{aligned} \tag{2}$$

$$\begin{aligned}
&\frac{\partial (h_1 h_2 D U_2)}{\partial t} + \frac{\partial}{\partial \xi_1}(h_2 D U_1 U_2) + \frac{\partial}{\partial \xi_2}(h_1 D U_2^{\,2}) + D U_1 (-U_1 \frac{\partial h_1}{\partial \xi_2} + U_2 \frac{\partial h_2}{\partial \xi_1}) \\
&= -f h_1 h_2 U_1 D - g D h_1 \frac{\partial \eta}{\partial \xi_2} + h_1 h_2 [- < wv(0) + wv(-1) >] \\
&- \frac{g D h_1}{\rho_0} \int_{-1}^{0} \int_{\sigma}^{0} [D \frac{\partial \rho'}{\partial \xi_2} - \frac{\sigma' \partial D}{\partial \xi_2} \frac{\partial \rho'}{\partial \sigma}] d\sigma' d\sigma + \frac{\partial}{\partial \xi_2} [2 \overline{A}_M \frac{h_1}{h_2} \frac{\partial U_2}{\partial \xi_2}] \\
&+ \frac{\partial}{\partial \xi_1} [\overline{A}_M D \frac{\partial U_1}{\partial \xi_2}] + \frac{\partial}{\partial \xi_1} [\overline{A}_M D \frac{h_2}{h_1} \frac{\partial U_1}{\partial \xi_1}]
\end{aligned} \tag{3}$$

In which, η is tidal level; D is total water depth; U_1、U_2 are depth-averaged velocity components in ξ_1, ξ_2 directions; h_1、h_2 are Lame coefficients; f is the Coriolis parameter; g is acceleration of gravity; -<*wu*(0)>,-<*wv*(0)> are wind stress components; -<*wu*(-1)>,-<*wv*(-1)> are bottom stress components; ρ is water density; $\rho' = \rho - \rho_0$; $\overline{A}_M = \int_{-1}^{0} A_M \, d\sigma$.

2.2 BASIC EQUATIONS OF INTERNAL MODE

Continuity equation:

$$\frac{\partial \eta}{\partial t} + \frac{1}{h_1 h_2} \frac{\partial (h_2 u)}{\partial \xi_1} + \frac{1}{h_1 h_2} \frac{\partial (h_1 v)}{\partial \xi_2} + \frac{\partial w}{\partial \sigma} = 0 \tag{4}$$

Momentum equations:

$$\begin{aligned}
&\frac{\partial (h_1 h_2 D u_1)}{\partial t} + \frac{\partial}{\partial \xi_1}(h_2 D u_1^{\,2}) + \frac{\partial}{\partial \xi_2}(h_1 D u_1 u_2) + h_1 h_2 \frac{\partial (w u_1)}{\partial \sigma} \\
&+ D u_2 (-u_2 \frac{\partial h_2}{\partial \xi_1} + u_1 \frac{\partial h_1}{\partial \xi_2} - f h_1 h_2) = -g D h_2 (\frac{\partial \eta}{\partial \xi_1} + \frac{\partial H}{\partial \xi_1}) \\
&- \frac{g D^2 h_2}{\rho_0} \int_{\sigma}^{0} [\frac{\partial \rho'}{\partial \xi_1} - \frac{\sigma'}{D} \frac{\partial D}{\partial \xi_1} \frac{\partial \rho'}{\partial \sigma'}] d\sigma' + \frac{h_1 h_2}{D} \frac{\partial}{\partial \sigma} [k_M \frac{\partial u_1}{\partial \sigma}] \\
&+ \frac{\partial}{\partial \xi_1} (2 A_M \frac{h_2}{h_1} D \frac{\partial u_1}{\partial \xi_1}) + \frac{\partial}{\partial \xi_2} [A_M \frac{h_1}{h_2} D \frac{\partial u_1}{\partial \xi_2}] + \frac{\partial}{\partial \xi_2} [A_M D \frac{\partial u_2}{\partial \xi_1}]
\end{aligned} \tag{5}$$

$$\frac{\partial(h_1h_2Du_2)}{\partial t}+\frac{\partial}{\partial\xi_1}(h_2Du_1u_2)+\frac{\partial}{\partial\xi_2}(h_1Du_2^2)+h_1h_2\frac{\partial(wu_2)}{\partial\sigma}+Du_1(-u_1\frac{\partial h_1}{\partial\xi_2}+u_2\frac{\partial h_2}{\partial\xi_1}+fh_1h_2)$$
$$=-gDh_1(\frac{\partial\eta}{\partial\xi_2}+\frac{\partial H}{\partial\xi_2})-\frac{gD^2h_1}{\rho_0}\int_\sigma^0[\frac{\partial\rho'}{\partial\xi_2}-\frac{\sigma'}{D}\frac{\partial D}{\partial\xi_2}\frac{\partial\rho}{\partial\sigma'}]d\sigma'+\frac{\partial}{\partial\xi_2}[A_M\frac{h_1}{h_2}D\frac{\partial u_2}{\partial\xi_2}] \quad (6)$$
$$+\frac{\partial}{\partial\xi_1}[A_M\frac{h_2}{h_1}D\frac{\partial u_2}{\partial\xi_1}]+\frac{\partial}{\partial\xi_1}[A_MD\frac{\partial u_1}{\partial\xi_2}]+\frac{h_1h_2}{D}\frac{\partial}{\partial\sigma}[k_M\frac{\partial u_2}{\partial\sigma}]$$

Concentration equation:

$$h_1h_2\frac{\partial CD}{\partial t}+\frac{\partial}{\partial\xi_1}(h_2u_1CD)+\frac{\partial}{\partial\xi_2}(h_1u_2CD)+h_1h_2\frac{\partial(wC)}{\partial\sigma}$$
$$=\frac{\partial}{\partial\xi_1}[\frac{h_2}{h_1}K_{\xi_1}D\frac{\partial C}{\partial\xi_1}]+\frac{\partial}{\partial\xi_2}[\frac{h_1}{h_2}K_{\xi_2}D\frac{\partial C}{\partial\xi_2}]+\frac{h_1h_2}{D}\frac{\partial}{\partial\sigma}[K_\sigma\frac{\partial C}{\partial\sigma}]-K_1Dh_1h_2C \quad (7)$$

Turbulence kinetic energy equations：

$$h_1h_2\frac{\partial(q^2D)}{\partial t}+\frac{\partial}{\partial\xi_1}(h_2u_1Dq^2)+\frac{\partial}{\partial\xi_2}(h_1u_2Dq^2)+h_1h_2\frac{\partial(wq^2)}{\partial\sigma}$$
$$=h_1h_2\{\frac{2K_M}{D}[(\frac{\partial u_1}{\partial\sigma})^2+(\frac{\partial u_2}{\partial\sigma})^2]+\frac{2g}{\rho_0}K_H\frac{\partial\rho}{\partial\sigma}-\frac{2Dq^3}{B_1\ell}\} \quad (8)$$
$$+\frac{\partial}{\partial\xi_1}(\frac{h_2}{h_1}A_HD\frac{\partial q^2}{\partial\xi_1})+\frac{\partial}{\partial\xi_2}(\frac{h_1}{h_2}A_HD\frac{\partial q^2}{\partial\xi_2})+\frac{h_1h_2}{D}\frac{\partial}{\partial\sigma}(Kq\frac{\partial q^2}{\partial\sigma})$$
$$h_1h_2\frac{\partial(q^2\ell D)}{\partial t}+\frac{\partial}{\partial\xi_1}(h_2u_1Dq^2\ell)+\frac{\partial}{\partial\xi_2}(h_1u_2Dq^2\ell)+h_1h_2\frac{\partial(wq^2\ell)}{\partial\sigma}$$
$$=h_1h_2E_1\ell\{\frac{K_M}{D}[(\frac{\partial u_1}{\partial\sigma})^2+(\frac{\partial u_2}{\partial\sigma})^2]+E_3\frac{g}{\rho_0}K_H\frac{\partial\tilde{\rho}}{\partial\sigma}\}\tilde{w}-h_1h_2\frac{Dq^3}{B_1} \quad (9)$$
$$+\frac{\partial}{\partial\xi_1}(\frac{h_2}{h_1}A_HD\frac{\partial q^2\ell}{\partial\xi_1})+\frac{\partial}{\partial\xi_2}(\frac{h_1}{h_2}A_HD\frac{\partial q^2\ell}{\partial\xi_2})+\frac{h_1h_2}{D}\frac{\partial}{\partial\sigma}(Kq\frac{\partial q^2\ell}{\partial\sigma})$$

Where, u_1, u_2, w are velocity components in ξ_1, ξ_2 and σ directions; C is the concentration of waste substance ; q^2, q^2l are the variables of turbulence kinetic energy; $k_{\xi_1}, k_{\xi_2}, k_\sigma$ are the diffusion coefficient of waste substance in ξ_1, ξ_2 and σ directions; k_1 is the disgraded coefficient of contaminant; the other variables are the same as above.

2.3 NUMERICAL COMPUTATION

In the numerical computation process, the technique of process-split is applied. The basic equations are discretized by the definite difference method, and staggered grid arrangement is used. The grid arrangement of external and internal mode is shown in Fig.1 and Fig.2 respectively. The semi-implicit solution TDMA method is used. On account of the different truncation error of the external and internal mode, the values of u, v are needed to regulate, moreover, the variable u, v shall be satisfied as follows: $\int_{-1}^{0} ud\sigma = U$ and $\int_{-1}^{0} vd\sigma = V$.

3. GRID LAYOUT AND COMPUTATIONAL CONDITION

3.1 GRID LAYOUT FOR SOUTH BRANCH ESTUARY

The computed range of south branch of the Changjiang Estuary is 91.70 kilometer in length and 1328.81 km^2 in area from Baimaokou to Hengsha Island outside. The body-fitted curvilinear mesh skill is used to fit for natural land boundary of south branch of the Changjiang Estuary and Changxing, Hengsha Island. The Layout of grid is shown in Fig.3. The number of grid allocation is 245×81×10 in ξ_1, ξ_2 horizontal and σ vertical direction respectively (Only printed every two meshes in Fig.3). The grid is densely scattered for the important computed Shidongkou region. In this area the minimum scale of longitudinal and transverse grid is 143.4 m and 56.6m respectively. Moreover the mesh scale is increased moderately in subordinate computational areas. According to practical water district, the

different roughness coefficient is selected. The value of roughness coefficient is between 0.018−0.026.

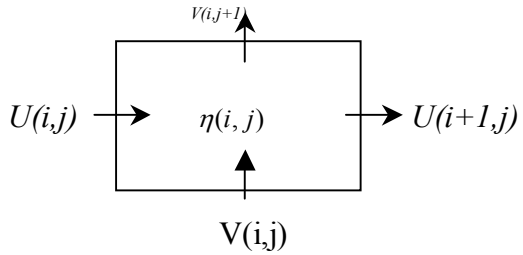

Fig. 1 Node arrangement of variables for external mode

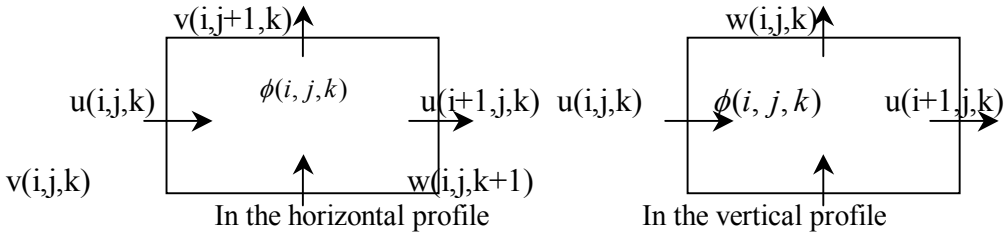

Fig. 2 Node arrangement of variables for internal mode

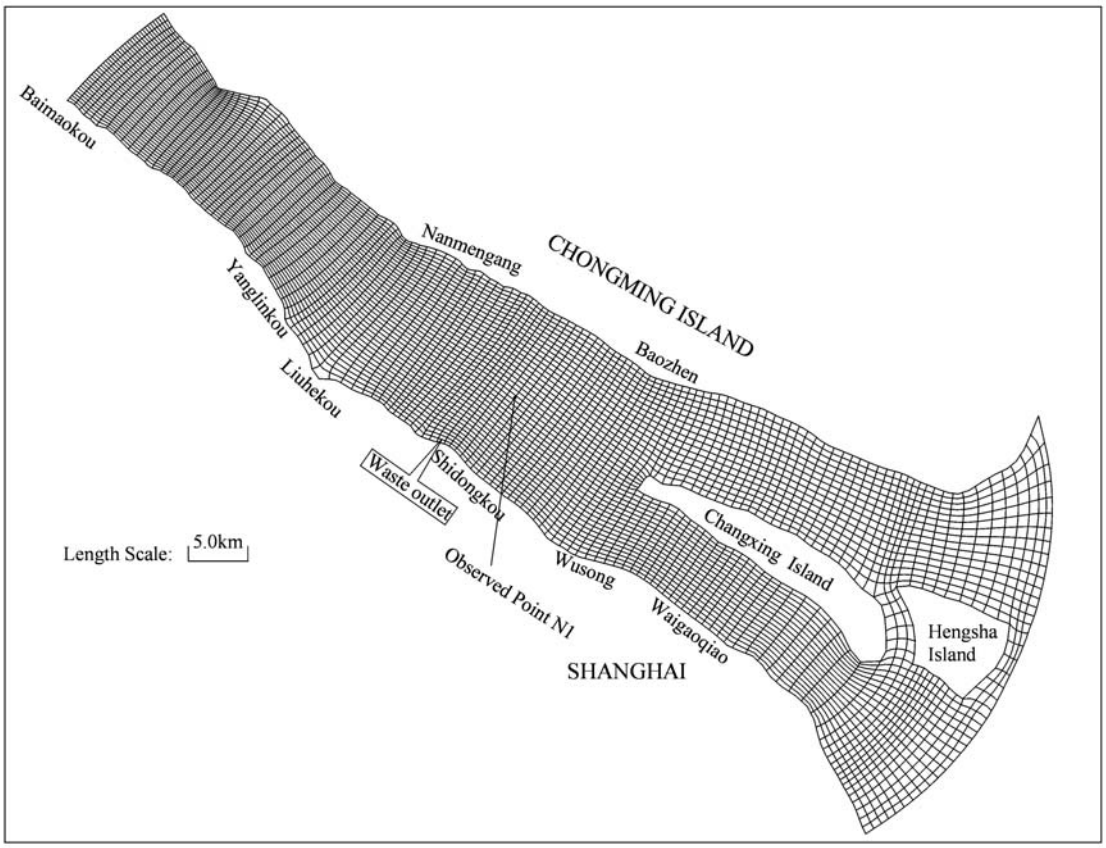

Fig. 3 Grid layout for the south branch of the Changjiang Estuary

• cal. — obs.

3.2 CONDITION OF WASTE DISCHARGE OUTLET

The Shidongkou waste discharge outlet belongs to Shanghai western district. Its location is shown in Fig.5, and its flow rate of waste discharge is 1.5×10^5 m^3/d, and the concentration of

COD_{cr} is 349mg/l. In water quality computation, The diffusion coefficient is formulated as follows: $k_{\xi_1} = \partial_{\xi_1} Du_*$; $k_{\xi_2} = \partial_{\xi_2} Du_*$; $k_\sigma = \partial_\sigma Du_*$.

In which, $\partial_{\xi_1}, \partial_{\xi_2}, \partial_\sigma$ is empirical coefficient; these values are 4.0, 0.5, 0.067 respectively; u_* is frictional velocity. The COD_{cr} disgraded coefficient k_1 is equal to 0.25 1/d.

4. COMPUTATIONAL RESULTS

The mathematical model is verified by the use of synchronous observed data of the Changjiang Estuary in Mar. 1996. Fig.4a−4b give the results of comparison between the calculated and the measured tidal elevation at Wusong and Nanmengang observed station. The figures show the model adequately reproduces the tidal elevations. The comparison between the computed and observed velocity of measured point N_1 in surface, middle, bottom layer is shown in Fig.5a−5c. The velocity distribution preferably accords with practical situation. Fig.6 shows the flow field for south branch of the Changjiang Estuary in surface, middle, and bottom layer at flood strength time, which also coincides well with the real. Fig.7 shows the pollutant COD_{cr} concentration distribution caused by Shanghai Shidongkou waste discharge in surface, middle and bottom layer at ebb strength time, and in Fig.7 the concentration isoline stands for 1%, 3% and 5% of effluent concentration. The polluted extent of water body is presented.

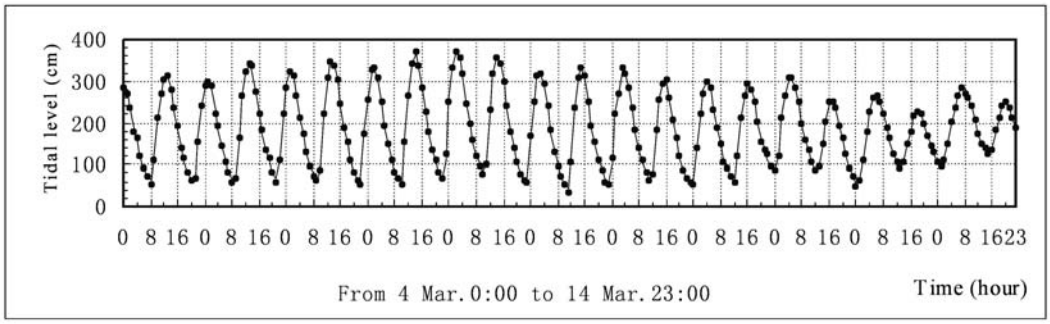

Fig. 4a Comparison of observed tidal level and calculational data (Wusong)

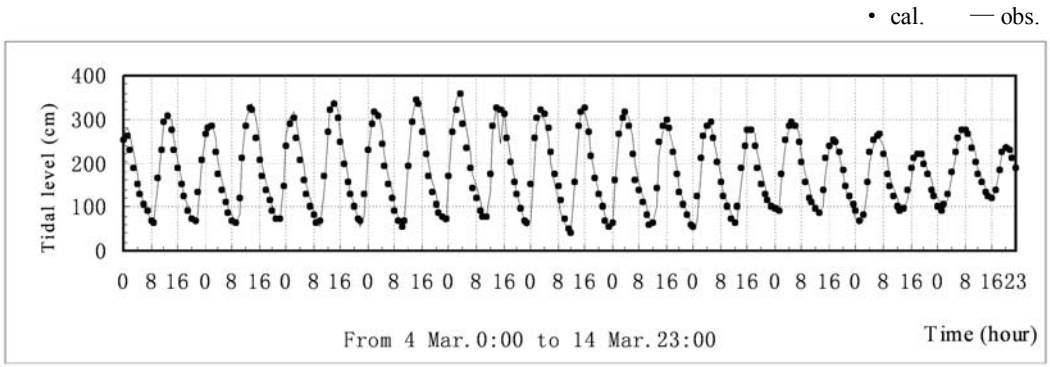

Fig. 4b Comparison of observed tidal level and calculational data (Nanmengang)

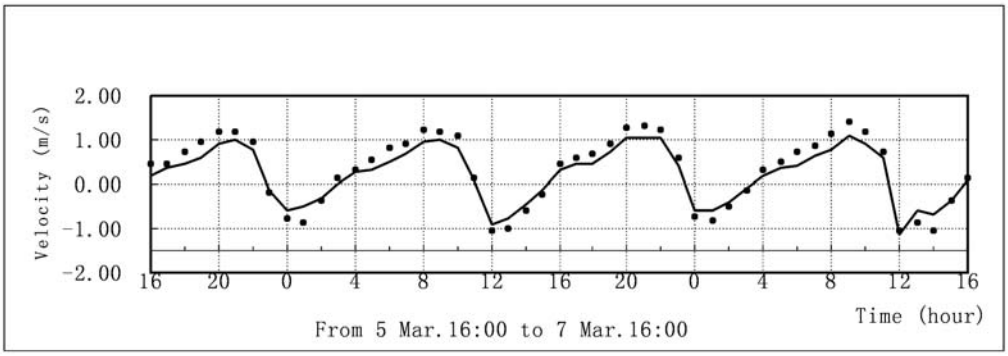

Fig. 5a Comparison of observed velocity and computational data (N1 Surface Layer)

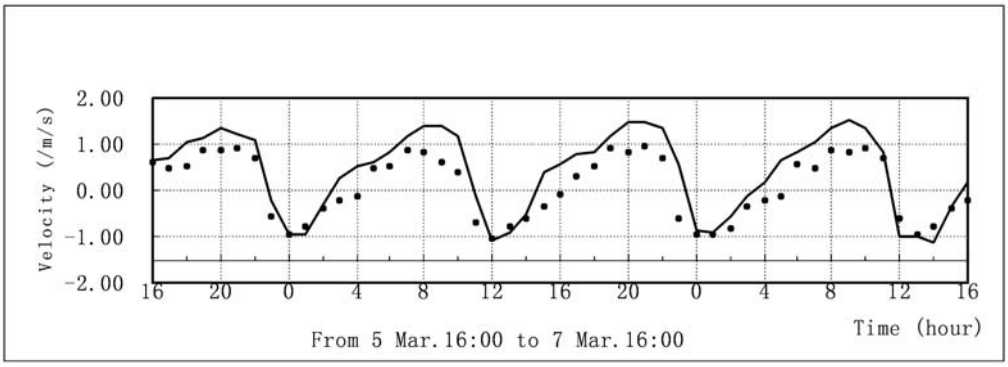

Fig. 5b Comparison of observed velocity and computational data (N1 Middle Layer)

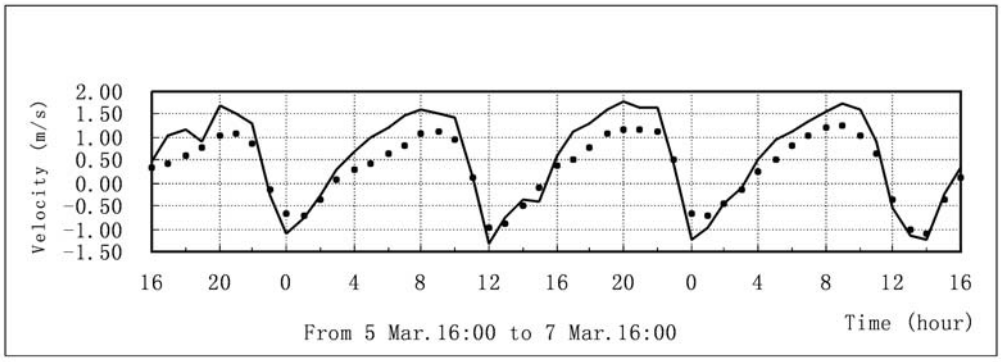

Fig. 5c Comparison of observed velocity and computational data (N1 Bottom Layer)

5. FINAL REMARKS

The hydrodynamic process and mass transportation of the Changjiang Estuary is complicated. In this paper the method of body-fitted curvilinear grid is applied to fit for irregular natural land boundary and islands, so that the precision of reflecting real boundary is enhanced. Based on curvilinear grid in plane and σ relative coordinate in vertical direction, A three-dimensional model of flow and pollutant transportation is established. During the process of numerical computation, the technique of process-split is used. The process of numerical solution is divided into the external mode and the internal mode based on POM Model. The external mode is used to solve fast process for surface gravity wave to gain water elevation and depth-averaged velocity, and the internal mode is applied to calculate slow process for gravity wave to obtain the characteristic of the three dimensional velocity of u, v, w. Simultaneously, the three dimensional polluted scope by Shidongkou waste discharge outlet is simulated. This work can be used to guide to waste pollution control in complex estuary region.

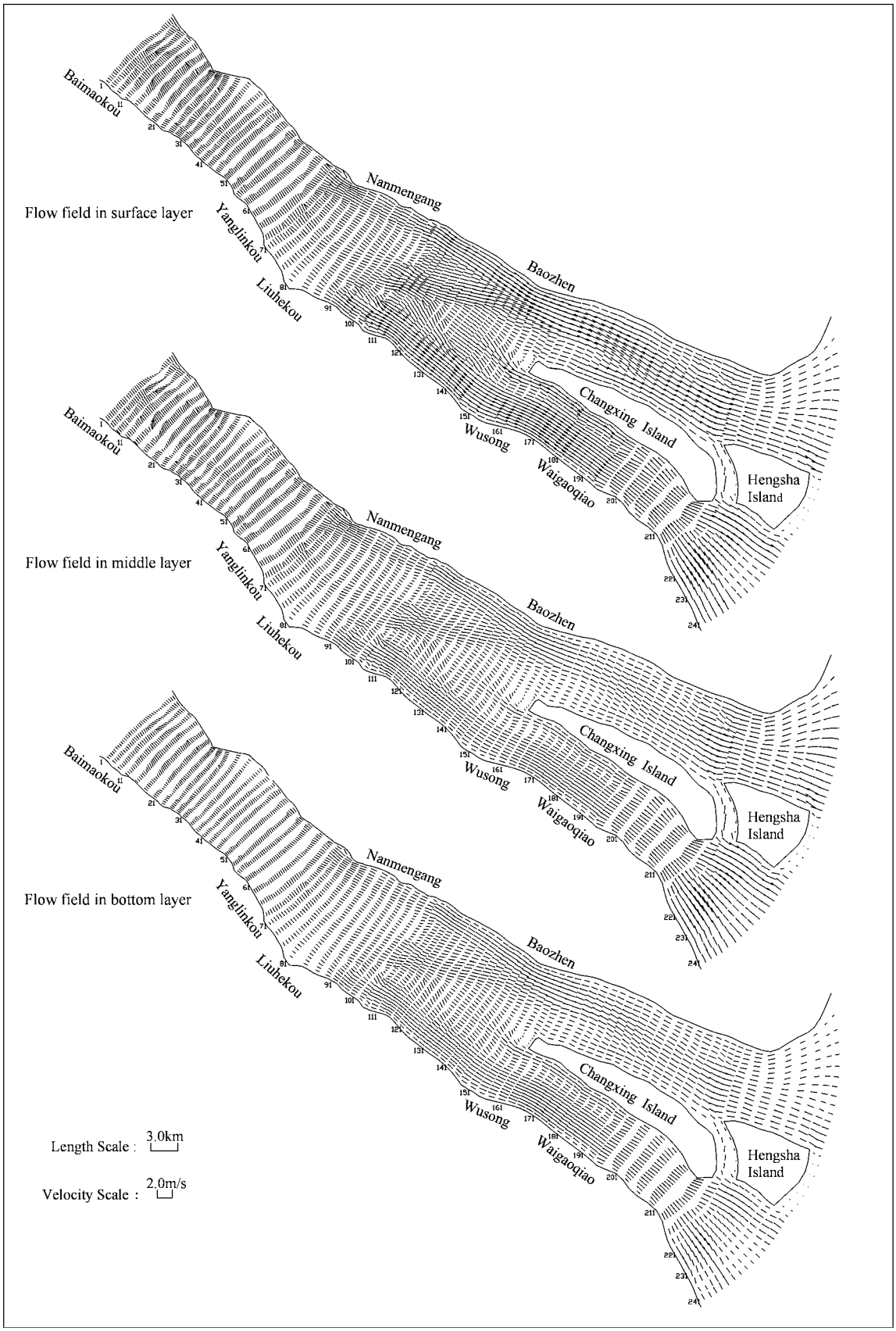

Fig. 6 The flow field at flood strength time

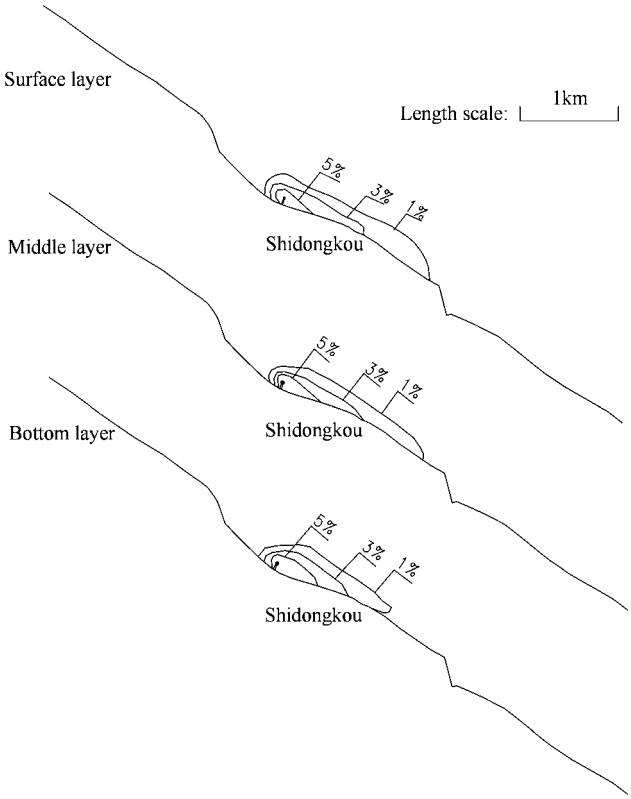

Fig. 7 The concentration field at ebb strength time

ACKNOWLEDGMENTS

This study is supported by The National Natural Science Foundation of China (Grant No: 50009001) and The Natural Science Foundation of Jiangsu Province (Grant No: BK2000004).

REFERENCES

L.-Y. Oey, G. L. Mellor, R. I. Hires, 1985. A Three-dimensional Simulation of Hudson-Raritan Estuary, Part I: Description of Model and Model Simulation. *J. Phys. Oceanogr.*, Vol.15, pp1676-1692.

A. F. Blumbreg, G. l. Mellor, 1987. A Description of A Three-dimensional Coastal Ocean Circulation Model, in Three-Dimensional Coastal Ocean Models, Vol.4, edited by N. Heaps, American Geophysical Union, Washington, D. C.

Alan F. Blumberg, George L.Mellor, 1983. Diagnostic and Prognostic Numerical Circulation Studies of the South Atlantic Bight. *Journal of Geophysical Research*, Vol.88, No.8, pp4579-4592.

Thompson J.F., 1982. Body-Fitted Coordinate Systems For Numerical Solution Of Partial Differential Equations. *J. Conput. Phys.*, Vol.47, pp1-108.

Jothi Shankar N, Hin-Fatt Cheong and Chun-Tat Chan, 1997. Boundary Fitted Grid Models for Tidal Motions in Singapore Coastal Waters. *J. of Hydraulic Research*, *IAHR,* Vol.35, No.1, pp3-19.

Sinous T. J, 1974. Verification of Numerical Models of Lake Ontario, Part I: Circulation in Spring and early Summer. *J.Pys.Oceanogr.*, No.4.

Y.S.Li, M.Y.Zhang, 1996. A Semi-implicit Three-dimensional Hydrodynamic Model Incorporating the Influence of Flow-dependent Eddy Viscosity, Bottom Topography and Wave-current Interaction. *Applied Ocean Research*, No.18, pp173-185.

Kang-Ren Jin, John H. Hamrick, Todd Tisdale, 2000. Application of Three-Dimensional Hydrodynamic Model for Lake Okeechobee. *Journal of Hydraulic Engineering, ASCE*, Vol.126, No.10, pp758-771.

E. A. Meselhe, F. Sotiropoulos, 2000. Three-dimensional Numerical Model for Open-channels with Free-surface Variations. *Journal of Hydraulic Research*, *IAHR,* Vol.38, No.2, pp115-121.;

Billy H. Johnson, Keu W. Kim, Ronald E. Heath, 1993. Validation of Three-Dimensional Hydrodynamic Model of Chesapeake Bay. *Journal of Hydraulic Engineering*, Vol.119, No.1, pp2-19.